

# Chiral symmetry in odd-odd neutron-deficient Pr nuclei

M.S. Fetea<sup>a</sup>, V. Nikolova, and B. Crider

Department of Physics, University of Richmond, Richmond, VA 23173, USA

Received: 2 January 2005 / Revised version: 22 April 2005 /

Published online: 21 July 2005 – © Società Italiana di Fisica / Springer-Verlag 2005

**Abstract.** We investigate the features of the electromagnetic transitions in the chiral  $^{132}\text{Pr}$  and  $^{134}\text{Pr}$  within the framework of particle rotor model, to understand why the measured  $B(M1)/B(E2)$  ratios for the yrare band are almost an order of magnitude larger than the corresponding ratios for the yrast band at low spins.

**PACS.** 21.60.Ev Collective models – 27.60.+j Properties of specific nuclei listed by mass ranges

A system is chiral if it is not symmetric with respect to a mirror reflection in any plane. Nuclear chirality [1] results from an orthogonal coupling of the angular momentum vectors in triaxial nuclei. The spontaneous symmetry breaking of the chiral symmetry manifests itself in a pair of degenerate bands [2]. The energy degeneracy between chiral doublets built on the same band structure, a nearly independent of spin  $S(I) = [E(I) - E(I - 1)]/2I$  for the chiral region, and the characteristic electromagnetic properties [3,4] are the experimental chiral fingerprints. Following the first example of a chiral nucleus,  $^{134}\text{Pr}$ , twelve chiral candidates have been found in odd-odd nuclei in the mass 130 region:  $^{126-132}\text{Cs}$ ,  $^{130-134}\text{La}$ ,  $^{132-134}\text{Pr}$ ,  $^{136}\text{Pm}$ ,  $^{138-140}\text{Eu}$ . Possible chiral pairs have been also reported in the even-odd  $^{135}\text{Nd}$  [5] and in the even-even  $^{136}\text{Nd}$  [6]. Recently, experimental work around the mass 100 region  $^{102-106}\text{Rh}$  [7] gives promising results. The best known example of a chiral doublet is provided by  $^{104}\text{Rh}$  [8].

The appearance of chiral bands is considered a strong evidence for the existence of triaxial deformations, since the chiral geometry cannot occur in an axially symmetric nucleus. In the mass 130 region, the chiral geometry is realized when the proton and neutron-hole occupy the lowest and the highest substates, respectively. The interplay of these tendencies towards elongated and disk-like shapes, may yield to a stable triaxiality [9].

Existing  $^{134}\text{Pr}$  calculations reproduce the staggering pattern for the  $B(M1)/B(E2)$  ratio for both the yrast and yrare bands and the  $B(M1)_{\text{in}}/B(M1)_{\text{out}}$  for the yrare band, but could not explain why for spins below  $16^+$ , the measured  $B(M1)/B(E2)$  ratios for the yrare band are almost an order of magnitude larger than corresponding ratios for the yrast band [10]. The calculated ratios for both the yrast and yrare bands are almost identical [10,11,12].

The aim of this work is to calculate the electromagnetic transitions in the chiral  $^{132}\text{Pr}$  and  $^{134}\text{Pr}$  using the Particle

Rotor Model (PRM). Although it lacks self-consistency, ignores the change in shape induced by rotation, and does not take into account the nucleus' polarization by the valence particles, the PRM uses wavefunctions having a good angular momentum and describes the system in the laboratory frame. Therefore the PRM directly yields the splitting between bands and the transition probabilities.

Even having lifetime measurements available, because the nuclei of interest are triaxial, the values of  $\varepsilon_2$  and  $\gamma$  cannot be extracted from the experimental data. The irrotational flow formula produces the largest moment of inertia with respect to the medium axes for  $\gamma = 30^\circ$ , which favors the aplanar orientation of the angular momentum. The value of  $\gamma$  practically does not influence the alignments of the valence particle and hole on the short and long axis, but these alignments are well defined only for sufficiently large values of deformation  $\varepsilon_2$  [13,14]. Calculations for  $^{132}\text{Pr}$  and  $^{134}\text{Pr}$  were performed for  $\gamma = 30^\circ$  and various values of  $\varepsilon_2$ . The values for the other parameters used in the calculations were:  $u_0 = -0.90$  MeV, and  $u_1 = -0.10$  MeV for the  $V_{np}$  interaction,  $gn_0 = 18.3$  and  $gn_1 = 7.0$  for the pairing strength, and  $\xi = 0.70$  and  $\eta = 1.0$  for the Coriolis attenuation.

The PRM calculations reproduce well the experimental [15,16,17] trend in excitation energies and the staggering pattern in energy splitting  $S(I)$ , in  $B(M1)/B(E2)$  for both chiral partners, and in  $B(M1)_{\text{in}}/B(M1)_{\text{out}}$  ratios. For the choice of parameters mentioned above, larger values of the  $\varepsilon_2$  (0.333) reproduce the  $\sim 300$  keV measured separation energy between the chiral bands. Smaller values of the  $\varepsilon_2$  (0.275) give closer values to the experimental  $B(M1)/B(E2)$  and  $B(M1)_{\text{in}}/B(M1)_{\text{out}}$  ratios in  $^{134}\text{Pr}$ . The calculated inband  $B(M1)$  for the yrast and yrare bands are shown in figs. 1 and 2, while the  $B(E2)$  are presented in figs. 3 and 4. As the spin increases, the  $B(E2)$  values within the two chiral partners become equal and slowly increase. The  $B(M1)$  show the characteristic

<sup>a</sup> Conference presenter; e-mail: mfetea@richmond.edu

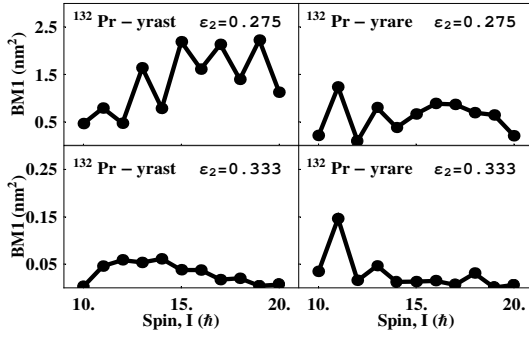


**Fig. 1.** The calculated yrast (left panels) and yrare (right panels)  $B(M1)$  vs. spin for  $^{132}\text{Pr}$ . The  $\varepsilon_2$  deformation parameters used were 0.275 (top panels) and 0.333 (bottom panels).

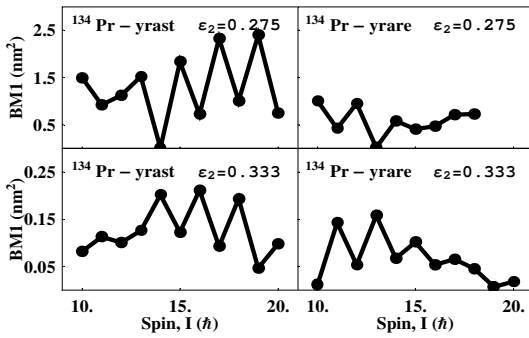


**Fig. 2.** The calculated yrast (left panels) and yrare (right panels)  $B(M1)$  vs. spin for  $^{134}\text{Pr}$ . The  $\varepsilon_2$  deformation parameters used were 0.275 (top panels) and 0.333 (bottom panels).

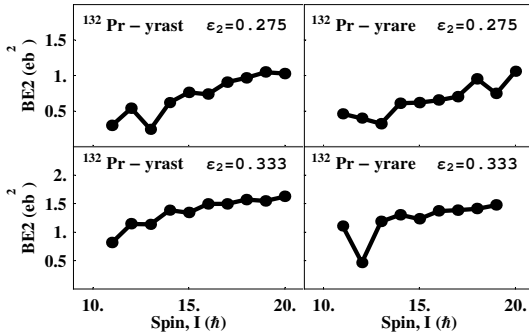


**Fig. 3.** The calculated yrast (left panels) and yrare (right panels)  $B(E2)$  vs. spin for  $^{132}\text{Pr}$ . The  $\varepsilon_2$  deformation parameters used were 0.275 (top panels) and 0.333 (bottom panels).

odd-even staggering, more pronounced at higher spins. This calculation indicates that for  $^{132}\text{Pr}$  the ratios for the yrare band are a factor of 2.0 and 2.5 smaller than for the yrast band with the  $\varepsilon_2$  values 0.333 and 0.275, respectively, and almost identical in  $^{134}\text{Pr}$ , for both  $\varepsilon_2$  values 0.333 and 0.275. Further, the calculation underestimates the experimental staggering in the  $B(M1)_{\text{in}}/B(M1)_{\text{out}}$  for  $^{134}\text{Pr}$  by a factor of 2.

The PRM calculations described above could not explain why in  $^{134}\text{Pr}$ , the measured  $B(M1)/B(E2)$  ratios for the yrare band are almost an order of magnitude larger than the corresponding ratios for the yrast band

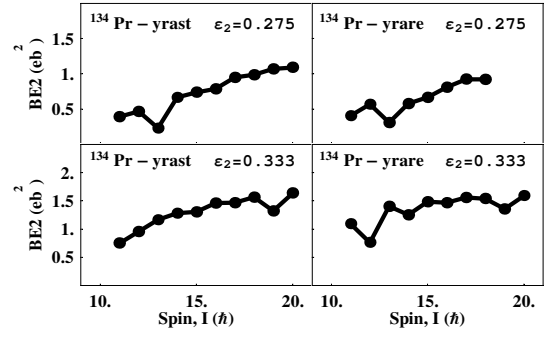


**Fig. 4.** The calculated yrast (left panels) and yrare (right panels)  $B(E2)$  vs. spin for  $^{134}\text{Pr}$ . The  $\varepsilon_2$  deformation parameters used were 0.275 (top panels) and 0.333 (bottom panels).

at low spins. Also, the values of  $\varepsilon_2$  that reproduce the  $\sim 300$  keV measured separation energy between the chiral bands and the energy splitting  $S(I)$  are large compared to the predicted values for the mass 130 region [18], and to the measured deformations in the neighboring nuclei. Smaller measured deformations than the sufficiently large theoretical values of  $\varepsilon_2$  needed to build a chiral geometry [13,14] may be the reason why the Pr nuclei are not the best known examples of chiral nuclei. Especially for weak pairing, the moments of inertia may deviate from the irrotational-flow values. More work is currently undertaken to find the influence other PRM-related parameters have on improving the theoretical understanding of the  $B(M1)$  and  $B(E2)$  for the chiral doublets in  $^{132}\text{Pr}$  and  $^{134}\text{Pr}$ .

This work was supported by the NSF Grant No. PHY 0204811 and Research Corporation Grant No. CC5494.

## References

1. S. Frauendorf, Rev. Mod. Phys. **73**, 463 (2001).
2. S. Frauendorf, J. Meng, Nucl. Phys. A **617**, 131 (1997).
3. S. Frauendorf, J. Meng, Nucl. Phys. A **557**, 259c (1993).
4. J. Peng *et al.*, Phys. Rev. C **68**, 044324 (2003).
5. S. Zhu *et al.*, Phys. Rev. Lett. **91**, 132501 (2003).
6. E. Mergel *et al.*, Eur. Phys. J. A **15**, 417 (2002).
7. P. Joshi *et al.*, Phys. Lett. B **595**, 135 (2004).
8. C. Vaman *et al.*, Phys. Rev. Lett. **92**, 032501 (2004).
9. L.L. Riedinger *et al.*, Acta Phys. Pol. B **32**, 2613 (2001).
10. K. Starosta *et al.*, in *Proceedings of the International Nuclear Physics Conference: Nuclear Physics in the 21st Century: INPC 2001, Berkeley, USA, 30 July-3 August 2001*, edited by E. Norman, L. Schroder, G. Wozniak, AIP Conf. Proc. **610**, 815 (2002).
11. S. Brant *et al.*, Phys. Rev. C **69**, 017304 (2004).
12. G. Rainowski *et al.*, Phys. Rev. C **68**, 024318 (2003).
13. K. Starosta *et al.*, Nucl. Phys. A **682**, 375c (2001).
14. K. Starosta *et al.*, Phys. Rev. C **65**, 044328 (2002).
15. C.M. Petrache *et al.*, Nucl. Phys. A **597**, 106 (1996).
16. S.P. Roberts *et al.*, Phys. Rev. C **67**, 057301 (2003).
17. T. Koike *et al.*, Phys. Rev. C **63**, 051301 (2001).
18. P. Möller *et al.*, At. Data Nucl. Data Tables **66**, 131 (1997).